Bioorganic & Medicinal Chemistry Letters 19 (2009) 6784–6787

Contents lists available at ScienceDirect

Bioorganic & Medicinal Chemistry Letters

journal homepage: www.elsevier.com/locate/bmcl

Lead optimization and structure-based design of potent and bioavailable deoxycytidine kinase inhibitors

Theodore C. Jessop [a,*], James E. Tarver [a], Marianne Carlsen [a], Amy Xu [a], Jason P. Healy [a], Alexander Heim-Riether [a], Qinghong Fu [a], Jerry A. Taylor [a], David J. Augeri [a], Min Shen [a], Terry R. Stouch [a], Ronald V. Swanson [c], Leslie W. Tari [c], Michael Hunter [c], Isaac Hoffman [c], Philip E. Keyes [a], Xuan-Chuan Yu [b], Maricar Miranda [b], Qingyun Liu [b], Jonathan C. Swaffield [b], S. David Kimball [a], Amr Nouraldeen [b], Alan G. E. Wilson [b], Ann Marie DiGeorge Foushee [b], Kanchan Jhaver [b], Rick Finch [b], Steve Anderson [b], Tamas Oravecz [b], Kenneth G. Carson [a]

[a] *Lexicon Pharmaceuticals, Princeton, NJ 08540, United States*
[b] *Lexicon Pharmaceuticals, The Woodlands, TX 77381, United States*
[c] *ActiveSite, San Diego, CA 92121, United States*

ARTICLE INFO

Article history:
Received 20 August 2009
Revised 21 September 2009
Accepted 22 September 2009
Available online 25 September 2009

Keywords:
Immunology
Virology
Cancer
Deoxycytidine kinase
Pharmacokinetics

ABSTRACT

A series of deoxycytidine kinase inhibitors was simultaneously optimized for potency and PK properties. A co-crystal structure then allowed merging this series with a high throughput screening hit to afford a highly potent, selective and orally bioavailable inhibitor, compound **10**. This compound showed dose dependent inhibition of deoxycytidine kinase in vivo.

As part of our GENOME5000 program, we have investigated the functions of nearly 5000 human genes by phenotypic analysis of the corresponding knockout (KO) mice.[1,2] The phenotype observed in deoxycytidine kinase (dCK) KO mice identified dCK as a potential drug target in multiple disease states within cancer, immunology and virology.[3] The connection between the nucleoside salvage pathway and these disease states has precedent.[4,5] Deoxycytidine kinase catalyzes the phosphorylation of pyrimidine and purine deoxynucleosides as well as various nucleoside analogs.[6–8] Although ubiquitously expressed, it is a nuclear enzyme with particularly high expression in lymphocytes.[7]

Crystal structures of dCK bound to various substrates are known.[9] We obtained a co-crystal structure of 5-fluorodeoxycytidine **1** in the substrate binding pocket of dCK (PDB code: 3IPX). The binding is characterized by extensive hydrogen bonding to the cytosine base and to the hydroxyl groups of the deoxysugar (Fig. 1). In addition to the residues that contribute to the hydrogen bonding network, the substrate binding pocket is further defined

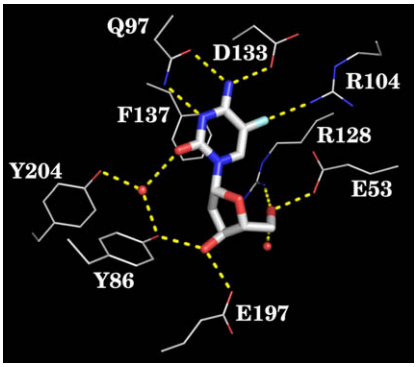

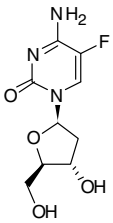

1

Figure 1. Schematic of the substrate binding site of dCK occupied by **1**; PDB code 3IPX.

* Corresponding author. Tel.: +1 609 466 6076; fax: +1 609 466 3562.
E-mail address: tjessop@lexpharma.com (T.C. Jessop).

0960-894X/$ - see front matter © 2009 Elsevier Ltd. All rights reserved.
doi:10.1016/j.bmcl.2009.09.081

by aromatic residues above and below the cytosine ring. Generally, the enzymatic specificity of dCK allows for a wide range of nucleosides to act as substrates.[7] Compound **1** was found to be a competitive inhibitor of dCK with an IC_{50} of 120 nM.

In designing new inhibitors of dCK, we sought to prepare non-substrate derivatives that utilized the dense network of hydrogen bonds available to the cytosine base. Towards this end, we synthesized cyclopentane analogs of **1** as deoxyribose surrogates that displayed improved hydrolytic stability. One of the early molecules that emerged from this approach was synthetic intermediate ester **5** (IC_{50} = 630 nM, Scheme 1) that prompted further investigation of aryl substitution.

Ester **5** was prepared by a three step sequence beginning with the palladium catalyzed π-allyl reaction of allylic acetate **3** with the sodium anion of 5-fluorocytosine to give an allylic alcohol in 80% yield. Hydrogenation afforded saturated alcohol **4** (quantitative yield) that was converted to **5** using the Martin Mitsunobu inversion. Treatment of alcohol **4** with *N*-Boc-sulfonamides under similar conditions followed by deprotection afforded phenyl sulfonamide analogs such as **6a** in low yields. Biphenylsulfonamides could be prepared by reaction of a bromophenyl sulfonamide with boronic acids under Suzuki conditions. Versatile intermediate amine **7**, prepared in 51% over three steps via a Boc-nosylate, was acylated with halogenated aryl acids that were then further elaborated to biphenyl analogs using Suzuki cross-couplings to give analogs **8a–e**, **10**.[10]

Replacement of the ester of **5** (IC_{50} = 630 nM) with a sulfonamide afforded 4-nitrophenylsulfonamide **6a** with improved chemical stability but approximately fivefold reduced activity. Removal of the nitro group gave the nearly equipotent **6b**. Biphenyl analogs afforded potencies superior to our initial lead **5**. Substitution at the 3-position was preferred to the 4-position (Table 1).

Although increasing the polarity of substituents generally had a modest effect on the IC_{50}, the effect on EC_{50} was dramatic (see

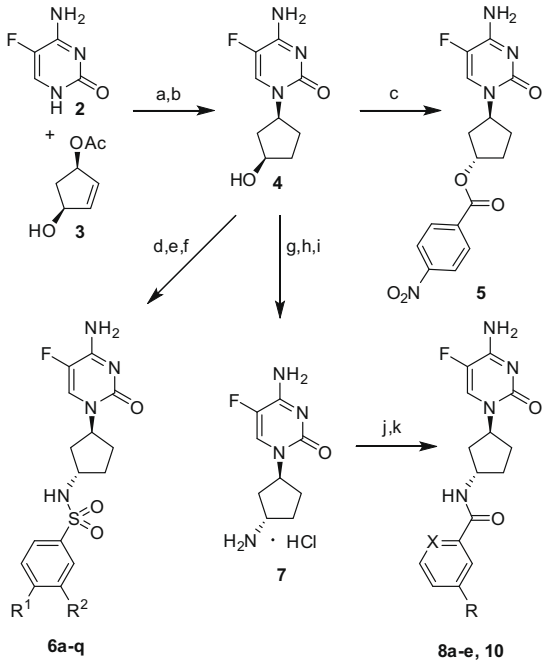

Scheme 1. Reagents and conditions: (a) (i) **2**, NaO*t*Bu, DMF; (ii) **3**, $Pd_2(dba)_3$, PPh_3, THF, 80%; (b) 10% Pd/C, H_2, MeOH (quant.); (c) PPh_3, DEAD, 4-nitrophenylbenzoic acid, THF, 66%; (d) *N*-Boc-sulfonamide, PPh_3, DEAD, THF; (e) TFA, DCM (2–23%, two steps); (f) boronic acid, Na_2CO_3, H_2O, CH_3CN, $Pd(dppf)Cl_2$ (10–70%); (g) BocHN-Ns, PPh_3, DEAD, THF; (h) PhSH, K_2CO_3, CH_3CN (51%, two steps); (i) HCl, dioxane, quant.; (j) 3-bromobenzoic acid (X = CH) or 4-bromopyridine-2-carboxylic acid (X = N), HATU, NMM, DMF or CH_3CN (54–60%); (k) boronic acid, $PdCl_2(dppf)$, Na_2CO_3, CH_3CN, H_2O (20–85%).

Table 1
In vitro and cell potency of phenylsulfonamides **6a–f** (see Scheme 1 for structures)

Compound no.	R^1 (4-position)	R^2 (3-position)	IC_{50}[a] (nM)	EC_{50}[b] (nM)
6a	NO_2	H	3200	16,000
6b	H	H	3600	17,000
6c	Br	H	2700	11,000
6d	Ph	H	350	5500
6e	H	Br	1900	2800
6f	H	Ph	120	600

[a] Inhibition of human dCK (IC_{50}) was determined using a lysate filter-binding assay.[11]
[b] Cell-based assay was a rescue assay that utilized inhibition of dCK to avoid dCK-mediated cytotoxicity of arabinoside C (Ara C).[11]

Table 2
In vitro and cell potency of *m*-biphenylsulfonamides **6g–s** (see Scheme 1 for structures)

Compound no.	R^1 (4-position)	R^2 (3-position)	IC_{50} (nM)	EC_{50} (nM)
6g	H	4-Methylphenyl	110	500
6h	H	4-Methoxyphenyl	64	300
6i	H	4-Cyanophenyl	49	390
6j	H	4-Methylsulfonyl	63	1800
6k	H	4-Aminocarboxy-phenyl	89	5900
6l	H	4-Carboxyphenyl	15,300	n.d.
6m	H	4-Chlorophenyl	51	240
6n	H	3-Chlorophenyl	79	360
6o	H	2-Chlorophenyl	45	430
6p	H	2,4-Dichlorophenyl	21	530
6q	H	4-Chloro-2-methylphenyl	21	290

Table 2). For example, methyl substituted **6g** and amide substituted **6k** have similar IC_{50} values (110 nM and 89 nM, respectively), however their EC_{50} values (500 nM and 5900 nM, respectively) are separated by more than 10-fold. This trend is illustrated in the polarities and potencies of **6g–k**. Charged analogs (as in **6l**) were not well tolerated. There was not a strong preference for substitution at any one position of the distal phenyl ring (as in **6m–o**) and di-substitution appeared to be preferred (as in **6p**, **6q**).

When substituents from the biphenylsulfonamide series (**6g–q**) were introduced onto a biphenylcarboxamide scaffold (see Table 3), the carboxamide analogs were generally more potent. Furthermore, frequent PK analysis of key analogs in mice allowed for simultaneous optimization of PK and potency. A comparative PK analysis was performed between the amide and sulfonamide series (see Table 4). The amide analogs **8b**, **8c** and **8e** were superior to the corresponding sulfonamides **6h**, **6m** and **6q**. In each instance, the amide analogs had lower clearance and lower volume of distribution while maintaining greater exposure and oral bioavailability.

While discovery efforts focused mainly on the amide series, a co-crystal structure was solved of dCK with the high-throughput screening[11] hit **9** (Fig. 2A; PDB code: 3IPY). Compound **9** bound dCK in a new pocket, formed by reorienting four amino acid side chains: Tyr 86, Tyr 204, Glu 196 and Glu 197. The biaryl region of **9** occupies the newly formed pocket with one pyrimidine nitro-

Table 3
In vitro and cell potency of *m*-biphenylamides **8a–e** (see Scheme 1 for structures; X = CH; R as shown below)

Ref no.	R	IC_{50} (nM)	EC_{50} (nM)
8a	Phenyl	260	910
8b	4-Methoxyphenyl	30	100
8c	4-Chlorophenyl	42	270
8d	3-Chlorophenyl	23	180
8e	4-Chloro-2-methylphenyl	21	170

Table 4
Mouse pharmacokinetics of biphenyl sulfonamides compared to biphenyl amides

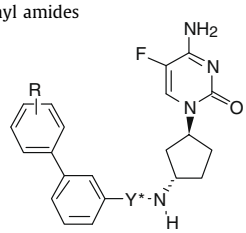

Compound no.	-R	Y*	AUC_{inf} (nM h)	C_{max} (nM)	$t_{1/2}$ (h)	t_{max} (h)	BA	Clearance (mL/min/kg)	V_z (L/kg)	IC_{50} (nM)	EC_{50} (nM)
6m	4-Cl	SO_2	5200	1000	2.1	2	nd	140	16	51	240
8c	4-Cl	C=O	15,800	16,200	0.8	0.3	12%	3	0.2	42	270
6h	4-OMe	SO_2	600	300	1.2	0.8	9%	63	4.4	64	310
8b	4-OMe	C=O	3800	3400	1.6	0.3	17%	18	1.3	30	100
6q	4-Cl, 2-Me	SO_2	2300	1500	1.6	0.3	15%	23	3	21	290
8e	4-Cl, 2-Me	C=O	10,800	10,100	1.3	0.3	58%	20	1.6	21	170
10	See Figure 3		22,000	7400	1.5	0.6	42%	7	0.8	1.7	17

Mice were dosed at 10 mpk po and 1 mpk iv and blood sampled to determine compound levels.
Clearance and volume were determined from the iv dose; other pharmacokinetic parameters utilized po dosing data. AUC_{inf}: Area under the curve (oral exposure) at infinite time; C_{max}: maximum concentration; $t_{1/2}$: half-life; t_{max}: time of maximum concentration; BA: bioavailability; V_z: volume of distribution from the terminal phase.

gen forming a water mediated hydrogen bond to Tyr 86. The upper portion of **9** sits in the pocket previously occupied by the cytosine base of **1**. The amide carbonyl of **9** appears to mimic the cytosine carbonyl of dC while lacking the multiple hydrogen bond interactions available with Gln 97, Asp 133 and Arg 104 (compare Fig. 2A and Fig. 1).

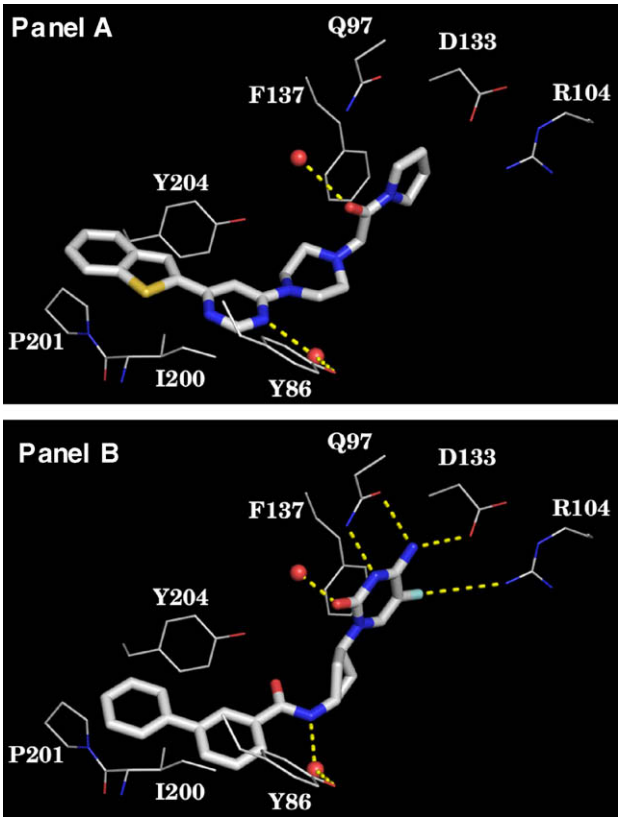

Figure 2. Panel A: Co-crystal structure of dCK and screening hit **9**; upper portion of **9** occupies some of the deoxycytidine binding pocket (compare Fig. 1) while the lower biaryl portion occupies a newly formed pocket; the ATP binding pocket (not shown) begins in the lower right corner of the panel; PDB code 3IPY. Panel B: Docking of **8a** from the *m*-biphenylamide series into the same binding site shown in panel A.

Docking biphenyl amide **8a** into this new X-ray crystal structure suggested that both **8a** and **9** might occupy common regions of the binding pocket (Fig. 2B). Compound **8a** appeared to form similar hydrogen bonding and π-stacking interactions as those seen between dCK and the cytosine base. In addition, the biaryl portion of **8a** resided in the newly formed hydrophobic pocket.

Compounds **8a** and **9** appeared to occupy the same region of the enzyme and share a similar shape, degree of flexibility and relative potency. Nonetheless, each compound seemed to derive much of its binding affinity through interactions with different parts of the enzyme. These characteristics compelled us to design a hybrid molecule (see Fig. 3) that would contain the complementary regions and binding features of the two molecules. Compound **8a** contained the highly functionalized cytosine base that could form a dense network of hydrogen bonds (Fig. 2B, upper region). Compound **9** lacked this hydrogen bonding network, yet retained good affinity for the enzyme presumably due to interactions of the pyrimidine and benzothiophene moieties with Pro 201, Ile 200, Tyr 204 and Tyr 86 (see Fig. 2, panels A and B). The designed hybrid **10** incorporated the upper region of **8a** and the lower region of **9** as seen in Figure 3.

Gratifyingly, compound **10** had an IC_{50} of 1.7 nM and EC_{50} of 17 nM. Further evaluation showed it to be stable to both human and mouse liver microsomes. Mouse pharmacokinetics of **10** were also quite favourable (see Table 4). The activity of **10** was measured in a panel of 75 in vitro assays. At a concentration of 10 μM, com-

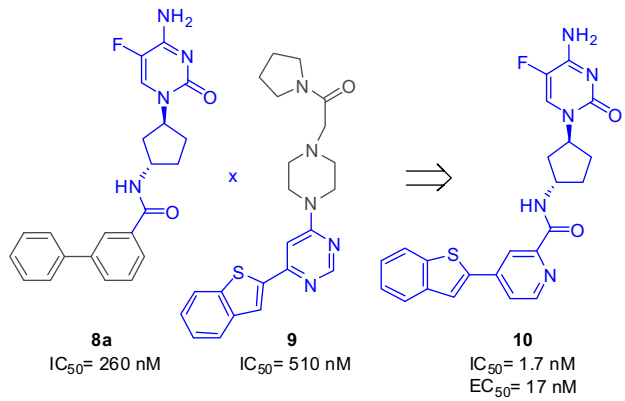

Figure 3. Design of hybrid molecule **10**. Functionality shown in blue was utilized in the design of hybrid molecule **10**.

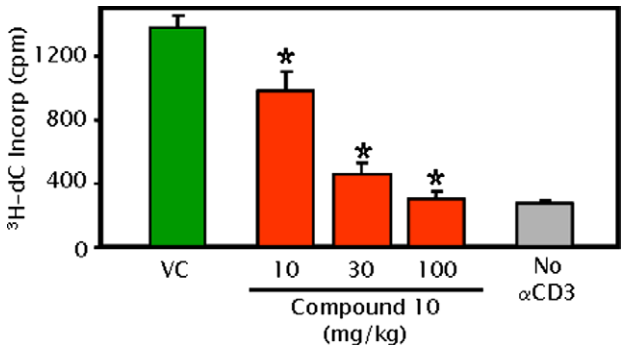

Figure 4. Compound **10** shows dose-dependent (10, 30, 100 mpk) inhibition of dCK activity in vivo. VC = vehicle control.

pound **10** showed less than 50% inhibition against all targets tested, except human Beta-2 and A2A.

The potency of **10** was also evaluated in primary mouse T cells. After stimulation of mouse splenic T cells with anti-CD3 and anti-CD28 antibodies, incorporation of ^{3}H-dC was measured.[12] Compound **10** inhibited the incorporation of ^{3}H-dC with an EC_{50} of 90 nM (human T cells) and 17 nM (mouse T cells). As expected, since deoxythymidine (dT) is not a substrate of dCK, incorporation of dT was not reduced after similar administration of **10**.

The ability of **10** to inhibit dCK in vivo was measured by reducing the incorporation of radiolabelled dC in mouse spleens after T cell stimulation.[13] Reduction of ^{3}H-dC incorporation was dose dependent and at a dose of 100 mpk, incorporation of ^{3}H-dC was reduced to the level observed without T cell stimulation (Fig. 4).

In summary, de novo design using 5-fluorodeoxycytidine **1** afforded submicromolar lead **5**. Concurrent optimization of potency and pharmacokinetics culminated in *m*-biphenylcarboxamides **8a–e**. Insights gained from X-ray co-crystal structures of **1**/dCK and **9**/dCK allowed the design of hybrid molecule **10**. Compound **10** was a potent, selective, and orally bioavailable inhibitor of dCK. Compound **10** also inhibited dCK both in primary T cells and in vivo.

Acknowledgements

The authors thank Alan Main and Giovanni Cianchetta for helpful discussions and assistance in manuscript preparation.

References and notes

1. Zambrowicz, B. P.; Sands, A. T. *Nat. Rev. Drug Disc.* **2003**, *2*, 38.
2. Walke, D. W.; Han, C.; Shaw, J.; Wann, E.; Zambrowicz, B.; Sands, A. *Curr. Opin. Biotechnol.* **2001**, *12*, 626.
3. Anderson, S., in preparation.
4. Carson, D. A.; Kaye, J.; Seegmiller, J. E. *Proc. Natl. Acad. Sci. U.S.A.* **1977**, *74*, 5677.
5. Joachims, M. L.; Marble, P. A.; Laurent, A. B.; Pastuszko, P.; Paliotta, M.; Blackburn, M. R.; Thompson, L. F. *J. Immunol.* **2008**, *181*, 8153.
6. Arner, E. S. J.; Eriksson, S. *Pharmacol. Ther.* **1995**, *67*, 155.
7. Bohman, C.; Eriksson, S. *Biochemistry* **1988**, *27*, 4258.
8. Gao, W. Y.; Shirasaka, T.; Johns, D. G.; Broder, S.; Mitsuya, H. *J. Clin. Invest.* **1993**, *91*, 2326.
9. Sabini, E.; Hazra, S.; Konrad, M.; Lavie, A. *J. Med. Chem.* **2007**, *50*, 3004. and references cited therein.
10. Augeri, D. J.; Carlsen, M.; Carson, K. G.; Fu, Q.; Heim-Riether, A.; Jessop, T. C.; Tarver, J.; Taylor, J. A. PCT Int. Appl. WO 2008076778 A1, 2008.
11. Yu, X. C.; Miranda, M.; Liu, Z.; Patel, S.; Nguyen, N.; Carson, K.; Liu, Q.; Swaffield, J. C. *J. Biomol. Screen.*, in press.
12. Radu, C. G.; Shu, C. J.; Nair-Gill, E.; Shelly, S. M.; Barrio, J. R.; Satyamurthy, N.; Phelps, M. E.; Witte, O. N. *Nature Med.* **2008**, *14*, 783.
13. Mice were dosed with compound by oral gavage beginning on day −1 relative to ip injection of anti-CD3 (0.5 μg/g body wt) antibodies. On day 0 mice received the second dose of compound followed by injection of anti-CD3, and a third dose of compound on day 1, followed by ip injection of 3H-dCTP (100 μCi/animal). Spleens were harvested from the mice on day 2, dissociated into single cell suspensions (based on spleen weights at 30 mg/ml), and a 25 μl aliquot of cell suspension harvested onto glass fibre filters and counted by liquid scintillation. $n = 6–8$ mice per group. The group receiving no anti-CD3 represents background 3H-dC incorporation ($n = 2$). $^*p < 0.05$ compared to vehicle control (VC).